CONF-780952--30

LA-UR -78-2481

TITLE: THE INITIATION AND PROPAGATION OF NORMAL ZONES IN A FORCE-COOLED TUBULAR SUPERCONDUCTOR

AUTHOR(S): J. K. Hoffer

SUBMITTED TO: 1978 Applied Superconductivity Conference
Pittsburgh, PA

los alamos
scientific laboratory
of the University of California
LOS ALAMOS, NEW MEXICO 87545

An Affirmative Action/Equal Opportunity Employer

Form No. 836 R2
St. No. 2629
1/78

DEPARTMENT OF ENERGY
CONTRACT W-7405-ENG. 36

THE INITIATION AND PROPAGATION OF NORMAL ZONES IN A FORCE-COOLED TUBULAR SUPERCONDUCTOR

J. K. Hoffer

ABSTRACT

A numerical analysis has been performed on the time-dependent equations of heat balance, gas convection, pressure drop, and mass-flow rate for supercritical helium gas flowing through a tubular superconductor. Three dimensional graphs of wall temperature, gas temperature, and mass-flow rate as functions of position and time are used to show the evolution of normal zones. In contrast to other methods of studying stability in superconductors by a quasi-steady-state analysis of critical-sized normal zones (minimum propagating zone), our analysis shows that stability is influenced by both the magnitude and the time dependence of the disturbance. As the current is increased in a system subjected to certain types of thermal disturbances, propagating normal zones may originate at positions well downstream from the site of the disturbance. At higher currents, propagating zones may originate both downstream and at the disturbed site, coalescing into a large propagating normal zone. With certain types of disturbances (such as an extraneous heat source over a short length of conductor), higher critical currents may be reached by fast current ramping, while with other types of disturbances (such as self heating in a degraded section of conductor), slow current ramping leads to higher critical currents.

I. NOMENCLATURE

Superconducting composite properties:
- outer diameter.....D_o
- temperature.....$T(x,t)$
- cross-sectional area.....a_s
- density.....ρ_s
- specific heat.....$c_s(T)$
- thermal conductivity.....$\kappa_s(T)$
- electrical resistivity.....ρ_e
- critical current.....$I_c(x,T)$
- total current.....I
- current shared by the stabilizing metal.....$I_s(x,T)$
- critical temperature.....$T_c(I)$

Coolant channel properties:
- perimeter.....U
- heat transfer coefficient.....$h(T,\Theta,P,m)$
- friction factor.....f
- hydraulic diameter.....D

Gas properties:
- temperature.....$\Theta(x,t)$
- pressure.....$P(\dot{m},f)$
- cross-sectional area.....a_g
- density.....$\rho_g(\Theta,P)$
- specific heat (at constant pressure).....$c_p(\Theta,P)$
- mass-flow rate.....$\dot{m}(x,t)$
- velocity.....$v(\dot{m},\rho_g)$
- viscosity.....$\eta(\Theta,P)$
- thermal conductivity.....$\kappa_g(\Theta,P)$
- Joule-Thompson coefficient.....$\mu(\Theta,P)$

Extrinsic properties:
- radiant heat flux to conductor.....$q(T)$
- extraneous heat rate.....$\gamma(x,t)$
- time.....t
- distance.....x

Subscripts:
- composite conductor.....s
- coolant gas.....g

Manuscript received September 28, 1978.

*Work performed under the auspices of the US Department of Energy. Los Alamos Scientific Laboratory of the University of California, Los Alamos, NM 87545

II. INTRODUCTION

The study of stability in a superconducting system seeks to determine whether a given disturbance in a current-carrying superconductor causes a normal zone to appear that subsequently grows in temperature or propagates with distance. Because it is difficult to predict the type or magnitude of a disturbance that might occur in a superconducting system, various authors have treated the problem of stability by assuming an initial temperature profile with a portion or all of the conductor in the normal or current-sharing state. The ensuing transient heat conduction problem has been avoided by some authors[1-5] by treating a critical-sized normal zone, that is, one that neither grows nor decays (the so-called minimum propagating zone), as a steady state or quasi-steady state (traveling wave) temperature distribution. Recently, Bejan and Tien[6] have studied the time-dependent problem, simplified to permit analytical solutions, to determine whether an initial disturbed profile subsequently would grow or collapse. Such studies have resulted in a variety of conservative stability criteria.

Superconductors have finite heat capacities, and thus normal zones do not appear instantaneously in superconducting systems when disturbed. A disturbance acts to initiate a temperature rise in all or a portion of the conductor, and, if it is sufficiently large, a normal (resistive) zone will be created. Except for very unique circumstances, stationary normal zones do not appear in a superconducting system. They either grow or shrink, depending on the current, the nature of the disturbance, and many other parameters. In this study we examine stability in a forced flow cooled tubular superconductor as might be found in a superconducting power transmission line. Using a numerical analysis technique, we solve the time-dependent equations of heat balance, gas convection, and conservation of mass, subject to a fixed pressure drop across the system. Terms dependent on time or position are added to the heat balance equation to simulate various thermal disturbances or, alternately, the superconducting parameters of the tube are assumed to be time or position dependent to simulate degradation.

III. MATHEMATICAL MODEL

This work represents an extention of previous studies[9-10] of cooldown and thermal wave propagation in uni-directionally force-cooled superconducting power transmission (SPT) cables. The codes developed for these studies have since been upgraded by including the mass conservation equation.[11] For our work, it was necessary to include a current-sharing Joule heating term and various extra terms or boundary conditions to simulate disturbances or superconductor degradation. Because the thermal processes we shall be studying propagate at speeds considerably less than the velocity of sound and because we choose <u>not</u> to follow pressure disturbances which propagate <u>at</u> the sound velocity, the equation for momentum conservation can be ignored. Also, the gas-flow velocities are sufficiently low that kinetic energy effects are negligible compared to enthalpy changes and can be ignored. The geometry we consider is that of straight tubular conductor in vacuum, cooled by supercritical helium gas passing though the

inside. The wall of the tube is a composite structure, which may be considered to be a homogeneous metal with physical properties identical to pure copper of high purity (residual resistivity ratio RRR=100), but displaying superconducting parameters nearly identical to that of Nb_3Sn. (By assuming various values of critical current density, any reasonably high ratio of copper to superconductor may be simulated.) The time-dependent equations for thermal balance in the composite conductor (tube wall), for thermal balance, pressure drop, and mass conservation in the gas stream then may be written as,

$$c_s \rho_s a_s \frac{\partial T}{\partial t} = \frac{\partial}{\partial x}\left(\kappa_s a_s \frac{\partial T}{\partial x}\right) - hU(T-\Theta) + \pi D_o \alpha + \rho_e I I_s / a_s + \gamma \qquad (1)$$

$$c_p \rho_g a_g \left(\frac{\partial \Theta}{\partial t}\right)_x = hU(T-\Theta) + \dot{m} c_p \left[\mu \frac{dP}{dx} - \left(\frac{\partial \Theta}{\partial x}\right)_t\right], \qquad (2)$$

$$\frac{dP}{dx} = -\frac{32 f \dot{m}^2}{\pi^2 \rho_g D^5}, \qquad (3)$$

and

$$\frac{\partial \dot{m}}{\partial x} = -a_g \frac{\partial \rho_g}{\partial t}. \qquad (4)$$

The terms on the r.h.s. of Eq. 1 represent the differential conduction heat, heat transfer to the coolant gas, radiant heat leak to the wall, Joule heating in the composite, and an extraneous heat term which is time and position dependent, all per unit length. Note that radial temperature gradients have been explicitly ignored. In Eq. 2, thermal conductivity in the gas has been ignored because it is trivial compared to that of the wall. However, values for the thermal conductivity are needed to evaluate the heat transfer coefficient h. The last two terms in Eq. 2 represent thermal changes due to the Joule-Thompson effect and gas convection. Equation 3 reflects our assumption that the pressure drop in the flow channel is due only to frictional effects.

We first solved the steady-state solution of Eqs. 1, 2, and 3, with $\gamma = 0$. The numerical steady-state solution was facilitated by combining Eqs. 1 and 2 to eliminate the heat transfer term and then assuming that $\Theta = T$. We neglected the term $a_s(\partial\kappa_s/\partial T)\cdot(\partial T/\partial x)^2$ which comes from expanding the thermal conductivity term in Eq. 1. After solving for $\Theta(x)$, we evaluated h, then calculated T(x) from Eq. 2. Then the r.h.s. of Eqs. 1-4 were evaluated for the time-dependent analysis. A forward-backward difference approximation was used to evaluate $\partial T/\partial x$ and $\partial\theta/\partial x$, and stability was insured by proceeding in very small time steps. It was necessary to calculate gas densities based on pressures obtained from the proceeding time step, as opposed to the usual method of calculating gas densities on the basis of pressures obtained from the proceeding distance step. This mathematical "trick" serves to impose a small but finite damping of pressure changes, which in the absence of momentum conservation (and hence an infinite speed of sound), would otherwise be free to intensify ad finitum with distance.

IV. PHYSICAL PARAMETERS

The geometry was chosen to match that of a 500-m length of 0.635-cm o.d. copper tubing, cooled by supercritical helium entering at $\Theta_0 = 10$ K and $P_0 = 10$ atm and exiting at $P_{500} = 1$ atm. However, we chose to follow only those events which occur in the first 3 m of the conductor, and hence $P_3 = 9.98$ atm, which yields a steady-state mass-flow rate $\dot{m} = 3.0$ g/s. Thus the following parameters were held constant throughout the computations.

$D_o = 0.635$ cm
$D = 0.480$ cm
$a_s = \pi(D_o^2 - D^2)/4 = 0.1357$ cm^2
$a_g = \pi D^2/4 = 0.1810$ cm^2
$U = \pi D = 1.508$ cm
$\rho_e = 8.9$ g/cm^3
$\Theta(0,t) = 10.0$ K
$P(0,t) = 10.0$ atm
$P(3m,t) = 9.98$ atm

All the remaining physical parameters had to be evaluated at each time and distance step. A distance step Δx of 4 cm was chosen to achieve sufficient resolution and a time step Δt of 0.002 s was then needed to insure accuracy and stability. Thus to follow an event lasting 1 s over the 3-m section of conductor involves 75 x 500 = 37,500 solutions of Eqs. 1-4, each with many changing physical parameters to be evaluated. To reduce computational time we developed very simple subroutines for computing these parameters, and generally we had to be satisfied with accuracies near 5%.

The specific heat of the composite c_s was assumed to be that of pure copper. However, since the temperatures in the normal zones often reached values well over 100 K, it was not sufficient to assume a simple cubic term for the lattice specific heat. Instead, a short Debye function routine was used,[12] based on a zero degree Debye theta value $\Theta_D = 310$ K for copper. We added to this a linear term to represent the electronic specific heat. Thus for $c_s(T)$,

$$c_s(T) = f(T/\Theta_D) + 6.28\cdot10^{-6}\, T \ (\mathrm{J/g\cdot K}). \qquad (5)$$

The thermal conductivity κ_s of copper was taken from Powell et al.[13] Their expression for the intrinsic resistivity ω_i was modified to give accurate values for κ_s up to 300 K, where $\kappa_{s,300\ K} \approx 4.0$ W/cm·K $\equiv 1/\omega_{i\infty}$. Thus our expression for κ_s for 4 K < T < 300 K is

$$\kappa_s(T) = 1/(\omega_i + \omega_o + \omega_{io}) \ (\mathrm{W/cm\cdot K}), \qquad (6)$$

where

$$\omega_i = \left[\frac{1}{16 + (1/1.9\ 10^{-6}\ T^{2.76})^2}\right]^{0.5},$$

$\omega_o = B/T$ and $B \equiv 1.0$ cm·K^2/W to correspond with the low temperature defect resistivity of copper with RRR = 100 (since $B \approx 100/RRR$), and

$$\omega_{io} = 0.5\,\omega_i\,\omega_o/(\omega_i + \omega_o).$$

Note that for temperatures lower than approx 40 K, $\omega_i = 1.9\cdot10^{-6}\ T^{2.76}$, which is identical with the expression given by Powell et al.

The electrical resistivity ρ_e of copper was obtained by fitting the copper alloy data of Clark et al.[14] Good fits over the range 4 < T < 300 K were obtained by the simple expression

$$\rho_e(T) = \sqrt{C_1 + C_2\ T^2} - C_3 \ (\Omega\ \mathrm{cm}), \qquad (7)$$

where for RRR = 100,

$C_1 = 8.4227\cdot10^{-13}$
$C_2 = 7.1580_5\cdot10^{-17}$
$C_3 = 9.0255\cdot10^{-7}$.

Only the value of C_3 needs to be changed to account for the RRR, according to the expression

$$C_3 = (\sqrt{C_1+C_2\cdot273^2} - RRR\cdot\sqrt{C_1+C_2\cdot4^2})/(1-RRR)$$

Equation 7 is more accurate for high values of the RRR but yields reasonably accurate values of $\rho_e(T)$ for RRR values as low as 5.

The superconducting parameters of the composite were based on measured values[6] of Nb_3Sn conductors in SPT geometries (self-field), where it was found that $T_c(I=0) = 17.0$ K and

$$I_c(T) = I_c(0 \quad (1 \quad ^{-2}/T_c^2), \qquad (8)$$

that is, a quadrati dence of critical current on temperature was obs For our computations, we have set $I_c(0) = 50$ ous the overall critical current density $J_c(0$ $7 \cdot 10^4$ A/cm^2. This corresponds roughly copper: Nb_3Sn - bronze ratio of 10:1. When the total current is greater than $I_c(T)$, $I_s = I - I_c(T)$.

The physical parameters of supercritical helium were obtained from analytical fits of the data of McCarty[15] over the limited temperature and pressure ranges of interest. Without attempting to justify the physical significance of the various terms, we list here the functions used and their applicability:

specific heat, accurate to ≈2% for $10 < \Theta < 300$ K and $1 < P < 10$ atm:

$$c_p(\Theta,P)\ (J/g\cdot K) = 5.191 + 18.5533\ \frac{(P - 0.5)}{(T-2)^2} \qquad (9)$$

density, accurate to ≈2% for $6 < \Theta < 300$ K and $1 < P < 5$ atm and accurate to ≈15% for $5 < P < 15$ atm if $\Theta \geq P$:

$$\rho_g(\Theta,P)\ (g/cm^3) = f(\Theta,P) \cdot P/R\Theta \qquad (10)$$

where

R = gas constant = 20.5016 cm^3·atm/g·K,

and

$$f(\Theta,P) = 1.00 + \left[153.66\ P(1.75 - T/30)\right]/T^4 \qquad (11)$$

Joule-Thompson coefficient, accurate to ≈20% for $10 < \Theta < 300$ K and $0 < P < 10$ atm:

$$\mu(\Theta,P)\ (K/atm) = [-0.045 + 133.2/(T+10)^2]\cdot$$

$$[1 + (50.635 \cdot (11-P)^{1/3} - 100)/T^2] \qquad (12)$$

viscosity, accurate to ≈10% for $5 < \Theta < 300$ K and $0 < P < 50$ atm:

$$\eta(\Theta,P)\ (g/cm\cdot s) = 10^{-6}\cdot[5.023T^{0.647} + 9.3\cdot (P-1)/T] \qquad (13)$$

thermal conductivity, accurate to ≈10% for $3 < \Theta < 300$ K and $1 < P < 25$ atm:

$$\kappa_g(\Theta,P)\ (W/cm\ K) = 1.5\cdot 10^{-4} + 4.0\cdot 10^{-6}\ T + 1.5\cdot 10^{-5}\ T^{1/2} + 7.0\cdot 10^{-5}\cdot (P-10)/T \qquad (14)$$

The steady-state heat transfer coefficient h for turbulent flow in helium has been evaluated from a modified Dittus-Boelter correlation as suggested by Yaskin et al.[16]

$$h = 0.023\ Re^{0.8} Pr^{0.4}\ (\Theta/T)^{0.5}\ \kappa_g/D \qquad (15)$$

where

$$Re = \dot{m}D/a_g\eta \quad \text{and} \quad Pr = c_p\eta/\kappa_g.$$

The friction factor f was taken to be 7% greater than that predicted by the correlation of Koo,[17] as a result of data obtained during helium flow experiments in copper tubing by Hoffer and Dean.[7] Hence,

$$f = 1.07\cdot(0.0014 + 0.125/Re^{0.32}). \qquad (16)$$

The radiant heat leak was also obtained experimentally[7] and is expressed as,

$$\alpha(T)\ (W/cm^2) = 5.23\cdot 10^{-4}\cdot(300-T)/300. \qquad (17)$$

The effect of this heat leak on the temperature rise along the conductor is not noticeable over the 3-m length studied here.

V. COMPUTER-SIMULATED DISTURBANCES

The first disturbance we examined is that of a short heat pulse, of magnitude 0.64 W/cm applied over a 50-cm length of the conductor from $0.5\ m < x \leq 1.0$ m, lasting 0.25 s. The heat is deposited entirely in the conductor and is distributed to the gas by heat transfer from the wall. At a current of 2200 A, a short normal zone is created in the downstream portion of the heated section after about 0.20 s (Fig. 1). At the end of the heating pulse, the normal zone recovers, and a thermal wave propagates downstream at a velocity $v_w = vc_p/(c_p+c_s)$ where $v = \dot{m}/\rho_g a_g$ is the coolant flow velocity. For these areas, $c_p/(c_p+c_s) = 0.9$ represents the fraction of the enthalpy increase due to both the heater and Joule heating in the normal zone that is carried by the gas in the traveling thermal wave. At 2250 A, shown in Fig. 2, the same heat pulse leads to slightly more Joule

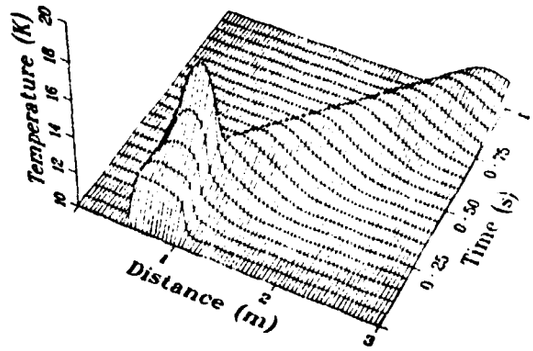

Fig. 1. Normal zone initiation and recovery at 2200 A following a heating pulse. Only the wall temperatures T (x,t) are shown.

heating in the normal zone. Recovery is not complete following the pulse, and the normal zone expands as the thermal wave moves downstream. ("Downstream" is a misnomer, because in the reference frame of the moving coolant, the heat pulse actually moves to the left.) The essential difference between the cases shown in Fig. 1 and Fig. 2 is that in Fig. 2, the gas in the heated section reaches temperatures just above T_c (2250 A) during the collapse of the heater-generated normal zone. A small but finite normal zone remains, now sustained by high gas temperatures, and the normal zone expands. At intermediate currents (2225 A), a smaller normal zone remains after the collapse of the heater-generated normal zone, then subsequently decays. This is due to the small but finite rate of damping of the thermal wave. There are two mechanisms for this thermal damping. First, thermal conductivity in the wall acts to diffuse the thermal wave. Secondly, the thermal wave in the gas and that in the wall are slightly out of phase, the gas wave leading that in the wall by several centimeters. Temperature differences T-Θ are highest at the peak in the wave, causing enhanced damping there. These increased temperature differences are caused in part by the Joule heating in the normal zone and in part by a reduction of the heat transfer coefficient because the mass-flow rate is reduced in the vicinity of the thermal wave, as

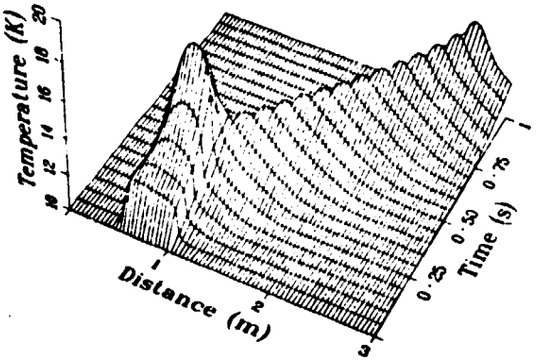

Fig. 2. Normal zone initiation and propagation at 2250 A due to a heating pulse.

seen in Fig. 3. The mass-flow effects lead to the assymetric shape of the traveling thermal wave, that is, cresting backwards, in agreement with actual observations.[9]

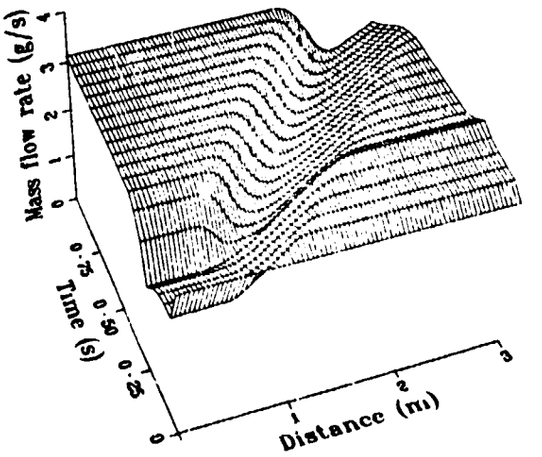

Fig. 3. Mass-flow rate for the case shown in Fig. 2.

In Figs. 4, 5, and 6, we examine the effects of a steady heat input on normal zone creation. For these cases, the heating level is identical to that described above, (0.64 W/cm over 50 cm), but the heater is not turned off after 0.25 s. As in Fig. 3, the initiation of heating causes a large change in local mass-flow rates. In Fig. 4, where I = 1950 A, a large normal zone is created and almost begins to propagate. However, just before runaway conditions are reached, the mass-flow rate recovers somewhat when the entire downstream section of conductor is no longer being heated. This allows the heat transfer coefficients to increase, and the normal zone collapses to a very small bump on the tip of the heated section. This is, in effect, a stationary normal zone sustained by the heater. At the 1960 A level in Fig. 5, just as the mass flow is starting to recover, gas temperatures downstream from the heater reach T_c (1960), a normal zone begins to develop, the mass flow rate is again upset, and a runaway condition ensues. Due to the finite size of the system being studied, the growing normal zone actually leaves the system after 3 s, and complete recovery occurs (except for the small normal zone under the heater, as in Fig. 4). Note that at approx 2 s, a second normal zone is created just

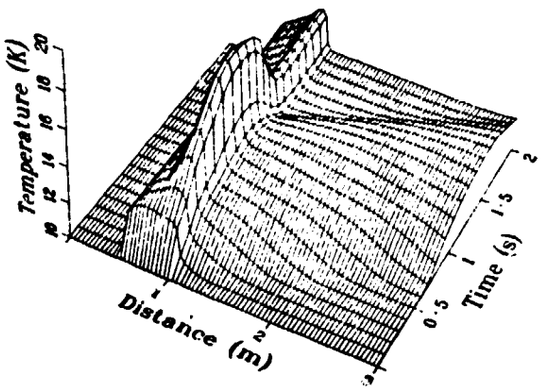

Fig. 4. Steady heating is initiated at t=0 for I=1950 A. The system relaxes to a steady state with the presence of a small normal zone.

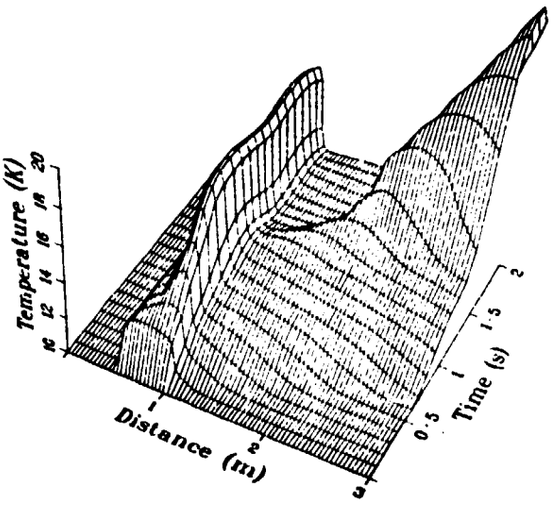

Fig. 5. At I=1960 A, a large normal zone is created which actually leaves the system, allowing recovery.

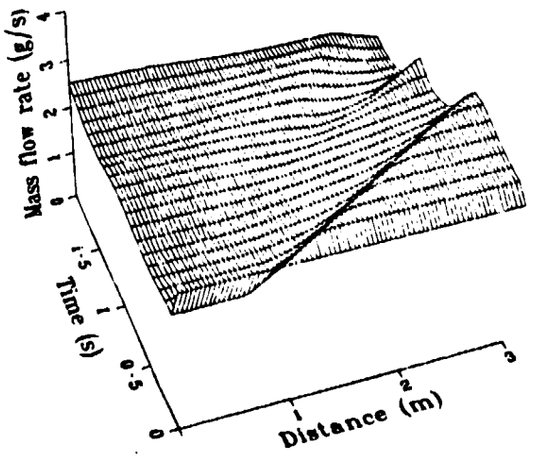

Fig. 6. The mass-flow rate for Fig. 5. Note the "waves" in $\dot{m}$ that occur due to subsequent normal zones eminating from the heated section. (See text).

downstream of the heater. Such multiple normal zone production, propagation, and escape may actually occur in very short systems. The complicated mass-flow "waves" for Fig. 5 are shown in Fig. 6.

The large upset in mass-flow rates that occur as the heater is turned on at t=0 acts to limit the current sustained by the superconductor. If the heater were already on before the current was introduced, higher currents could be reached before propagating normal zones develop, as shown in Figs. 7 and 8. For these cases, the heater is "on" at all times, and at t=0 the current is suddenly increased from $I_{initial}$ to I_{final}. The mass-flow rates are not noticeably upset by the current rise, and higher currents can be reached. Note the inaccuracy in the initial steady-state temperature profile due to our having ignored the term in $\partial k_s/\partial T$. In Fig. 7, where I_{final}=2050 A, a sizeable stationary normal zone has been created under the heater. Increasing the current further from 2050 A to 2080 A in Fig. 8, causes this normal zone to grow to proportions that can no longer be sustained by the coolant, and a large normal zone begins to propagate. In another example, where $I_{initial}$ = 0 and I_{final} = 2080 A, a propagating normal zone also

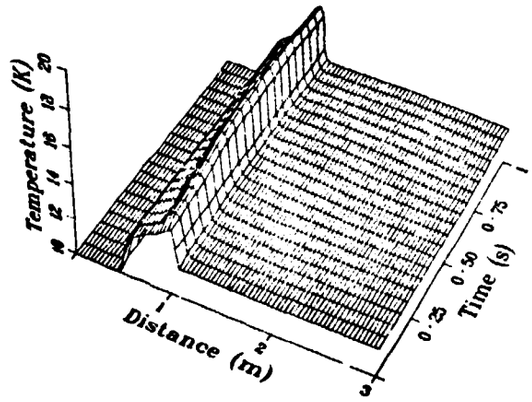

Fig. 7. The heater is on prior to and after t=0, but the current is suddenly increased from I=0 to I=2050 A at t=0.

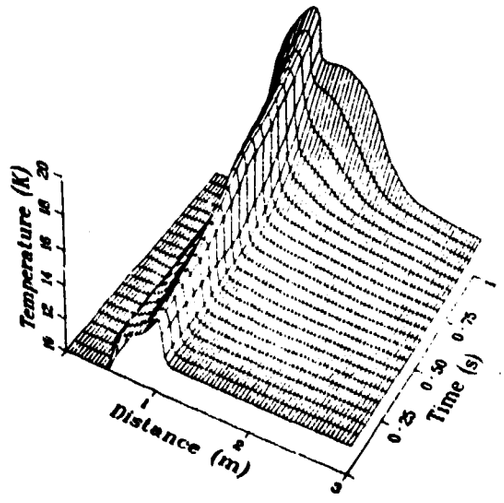

Fig. 8. At t=0, the current is increased from 2050 A to 2080 A. The heater has been "on" at all times.

developed. However, it did not develop as quickly because there was no self-Joule heating present at t=0. Thus we propose that if one were measuring critical current in a force-cooled superconducting system in which a local steady heat source were present, fast current ramping might give rise to higher measured critical current values.

Of course, we have not attempted to conjecture what might be the parallel of the "heater" in an actual superconducting system. Therefore we proceed with a more realistic disturbance, caused by a degraded section of superconductor. We assume now that over the section $0.5 < x \leq 1.0$ m, the superconductor has been somehow degraded such that $T_c(I=0) = 17$ K as before, but $I_c(0) = 2500$; thus over the degraded section, the critical current is only one-half the value in the undegraded sections. At t=0, the current is suddenly increased from $I_{initial}$ to I_{final}. If the critical current is exceeded in the degraded section, self-Joule heating takes place. However, due to current sharing in the degraded section, the magnitude of the Joule heating increases slowly with time so that the upset in mass-flow rates is not as drastic as if a "heater" had been suddenly turned on as in the case of Fig. 5. Hence in Fig. 9, where $I_{initial}$=0 and I_{final}=2550 A, a heated normal zone first grows slightly, but, when the mass-flow rate equilibrates, relaxes to a stationary state, sustained by self-Joule heating. However, in Fig. 10, where $I_{initial}$=0 and I_{final}=2565 A, the mass-flow rate has not quite equilibrated before

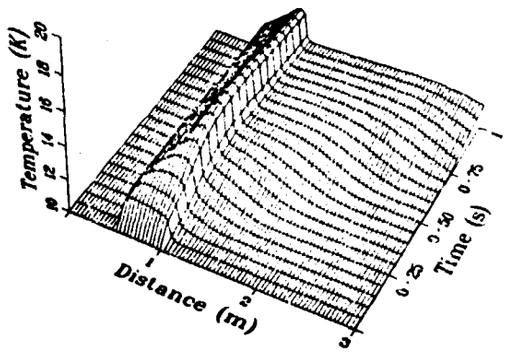

Fig. 9. The origination of stationary normal zone sustained by self-Joule heating in a degraded section of superconductor. At t=0, the current is increased from 0 to 2550 A.

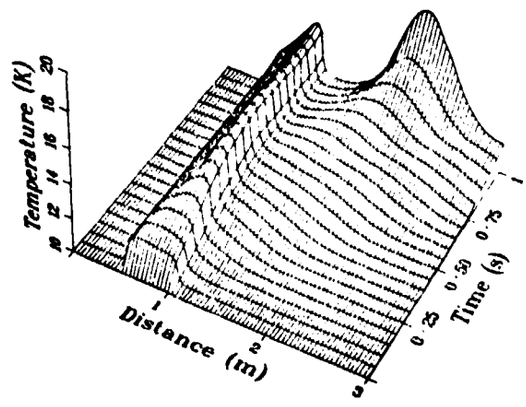

Fig. 10. The origination of a propagating normal zone due to an upstream degraded section. At t=0, the current is increased from 0 to 2565 A.

downstream gas temperatures reach T_c in the undegraded superconductor and a new normal zone appears and propagates in the undegraded superconductor. Figure 11 shows that mass-flow effects are present in this case, where $I_{initial}$=2500 and I_{final}=2565 A. Here, the small increase of current leads to but a a small upset in $\dot{m}$, and 2565 A can be sustained by the system. Under such conditions, slow current ramping would lead to higher measured critical currents. However, if one were searching for degraded sections of superconductor, he easily might be misled by the large normal zone originating downstream from the actual degraded section, since this might be the only measurable or detectable voltage drop in the system.

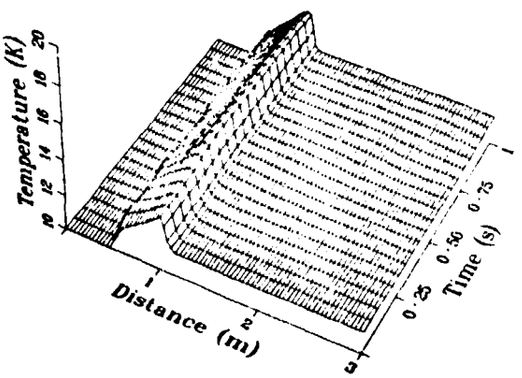

Fig. 11. When the current is increased from 2550 A to 2565A at t=0, mass-flow rates are less upset, and no normal zones appear in the undegraded sections.

REFERENCES

1. W. H. Cherry and J. I. Gittleman, Solid State Electronics 1, 287 (1960).
2. L. Dresner, IEEE Transactions on Magnetics, Vol. MAG-13, 670 (1977).
3. B. J. Maddock, G. B. James and W. T. Norris, Cryogenics 9, 261 (1969).
4. L. Dresner, Cryogenics 16, 675 (1976).
5. M. N. Wilson, "Whose Afraid of Force Flow Conductors?" Research Note #SMR/37, Rutherford High Energy Laboratory, Chilton Didcot Oxfordshire, May 1978.
6. A. Bejan and C. L. Tien, ASME Heat Transfer Conference, Salt Lake City, Utah, August 1977. Paper 77-HT-74.
7. J. K. Hoffer, E. C. Kerr, and W. C. Overton, Jr., IEEE Transactions on Magnetics MAG-13, 408 (1977).
8. F. J. Edeskuty, "DC Superconducting Power Transmission Line Project at LASL, USERDA Division of Electrical Energy Systems, Progress Report #15," Los Alamos Scientific Laboratory, LA-6699-PR
9. J. K. Hoffer and J. W. Dean, ASME Heat Transfer Conference, Salt Lake City, Utah, August 1977, Paper 77-HT-76.
10. D.C. SPTL Project at LASL, USERDA Division of Electrical Energy Systems, Progress Report #19, Los Alamos Scientific Laboratory, LA-7116-PR.
11. D.C. SPTL Project at LASL, USERDA Division of Electrical Energy Systems, Progress Report #21, Los Alamos Scientific Laboratory.
12. J. E. Kilpatrick and R. H. Sherman, Los Alamos Scientific Laboratory LA-3114 (1964).
13. R. L. Powell, H. M. Roder, and W. J. Hall, Phys. Rev. 115, 314 (1959).
14. A. F. Clark, G. E. Childs, and G. H. Wallace, Cryogenics 10, 295 (1970).
15. R. D. McCarty, US Nat. Bureau of Standards Tech. Note 631, (1972).
16. L. A. Yaskin, M. C. Jones, V. M. Yeroshenko, P. V. Giarratano, and V. D. Arp, Cryogenics 17, 549 (1977).
17. E. C. Koo, D. Sci. Thesis in Chemical Engineering, Massachusetts Institute of Technology, 1932.